Proceedings of the ASME 2025 44th International Conference on Ocean, Offshore and Arctic Engineering
OMAE2025
June 22-27, 2025, Vancouver, British Columbia, Canada

OMAE2025- 157489

CONSISTENCY ASSURANCE BETWEEN ILA AND STRUCTURAL MODEL IN TIME-DOMAIN STRUCTURAL ANALYSIS FOR FLOATING OFFSHORE WIND TURBINE

Youjin Yim
Front Energies
Houston, Texas

Hyungtae Lee
Front Energies
Houston, Texas

Johyun Kyoung
Front Energies
Houston, Texas

Jang Kim
Front Energies
Houston, Texas

Laurent Mutricy
Sofresid Ekium
Nantes, France

Raffaello Antonutti
Sofresid Ekium
Nantes, France

Alexis Martin
Sofresid Ekium
Brest, France

ABSTRACT

Most of a floating wind substructure's life will be spent with the turbine in production, largely determining loading regimes. In this condition, system mechanics are strongly coupled; hence, a good structural stress prediction can only derive from time-domain coupled Integrated Load Analysis (ILA). Experience shows that fatigue governs the design of major structural components and must thus be incorporated into the process early and robustly. With the many design load cases involved and the need to process time series in full to compute damage, a calculation process quickly going from ILA to local structural stresses is essential. This is the aim of the presented response-based methodology.

Enhancing the reliability of response-based time-domain analysis for Floating Offshore Wind Turbines (FOWTs) requires rigorous verification of all considered load components such as wind, wave, current loads, inertia, mooring, and Morison forces. Since the time-domain structural analysis is closely related to the ILA for the external environments and platform response for structural response assessment, ensuring consistency between the ILA and structural modeling of FOWTs is crucial. Therefore, ILA model should incorporate consistent geometric and dynamic properties from structural model, and the structural model should accurately incorporate all loads from the ILA. Once the consistency is achieved, theoretically the total resultant force at boundary conditions should converge to zero.

This paper presents a validation for load recovery and its influence on the structural response in the time domain. As an application, structural analysis of a conventional semisubmersible FOW platform supporting a 15 MW turbine is performed utilizing both open-source (OpenFast) and commercial (OrcaFlex) software for integrated load analyses. Recovered wind, wave and current loads as well as other resultant forces are thoroughly analyzed to ensure load balance and verify whether they have been accurately considered in the structural analysis. The present study shows the importance of load balance to ensure the reliability of response-based time-domain structural analysis; this feeds into the ability to reach substructure design convergence and optimization in an acceptable timeframe, ultimately decreasing risk and improving the chances of project success.

Keywords: load balance, FOWT, response-based time domain structural analysis

NOMENCLATURE

3P/6P	Synchronous blade passing frequencies
det [·]	Determinant of a matrix
DLC	Design Load Case
DOF	Degrees Of Freedom
N_{FE}, N_{ILA}	DOF in FEA and ILA
FD	Frequency Domain
TD	Time Domain
FE	Finite Element
FEA	Finite Element Analysis
FFT	Fast Fourier Transformation
IFFT	Inverse FFT
FOW	Floating Offshore Wind
ILA	Integrated Load Analysis
$\boldsymbol{M_{FE}}, \boldsymbol{K_{FE}}$; $\boldsymbol{M_{ILA}}, \boldsymbol{K_{ILA}}$	Mass and stiffness matrices in FEA and ILA
$\boldsymbol{R}$	Transformation matrix between displacement vectors in FEA and ILA
$\boldsymbol{u_{FE}(u)}, \boldsymbol{u_{ILA}}$	Displacement (linear and angular) vectors in FEA and ILA
VM	von Mises

1. INTRODUCTION

Floating wind substructure engineering requires a different mindset compared to offshore oil & gas. Alongside the serial fabrication and installation topics, absent in the conventional floating offshore platform space, these structures must be designed to host a very lively payload: a large wind turbine generator.

A narrow vision of a floater withstanding the static burden of a topside, perhaps subjected to a peculiar wind load, is far from reality: turbine operation-related loads are prevalent and also quite sensitive to delicate parameters such as mechanical flexibility, structural damping, and controls, all well outside the conventional floating structure design workflow. Furthermore, in power production conditions system mechanics are strongly coupled; hence, a proper structural response prediction can only derive from time-domain coupled analysis. This makes coupled simulation-based structural assessment (since the early phases) necessary for design convergence and risk and cost minimization, with fatigue being the main challenge.

1.1 Fatigue in floating wind

Similarly to classic floating offshore platforms, FOW structures undergo cyclic loading throughout their operational life due to waves and wind, generating fatigue. On top of this, the presence of a large WTG, expected to operate (power production) throughout most of design life, introduces a completely new loading regime imposing a radical mindset change compared to conventional floating platform design. The following TABLE 1 summarizes the causes of this paradigm shift.

TABLE 1: Loads on FOW Structure

Physics	FOW loads	FOW responses	Conventional floating platforms
Marine	Wave, current, mooring loads comparable		
Wind	Intense and sensitive to turbulence	Large low-freq. cycles including gravity loads under tilt	Way less sensitive to wind details
Vibrations	Aero-servo loads, esp. 3P and 6P	Elastic vibrations in tower and primary floater structure	No significant vibrations outside ringing / springing
Inter-dependency through controls	Coupled through WTG controls and moving parts, wind and wave dynamics interdependent		Decoupled loading processes, wave-dominated

The consequence is that in FOW fatigue becomes simultaneously prevalent and more complex to predict. Fatigue loads must now be derived from coupled time-domain simulations (FIGURE 1) as early as possible, and typically since the conceptual stage for meaningful design choices. Mainstream norms and guidance notes including IEC [1], DNV [2], [3], and BV [4], stress out this requirement.

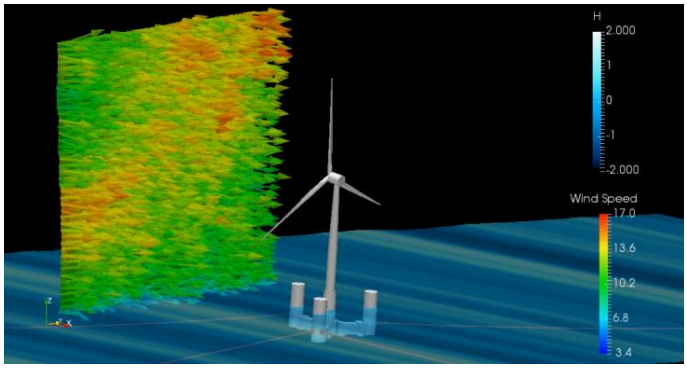

FIGURE 1: Visuals of a coupled aero-hydro-servo-elastic simulation.

1.2 Marine component design

Oil & gas structure designers often consider fatigue to be a local issue to be treated at a late stage. This is no longer applicable to FOW because of a combination of the following facts:

- Fatigue governs large parts of the substructure along with their design philosophy, such as a semi-submersible's main column and transition piece, but also mooring lines: turbine vibrations can and do travel through the floater and station-keeping system, exciting any local modes e.g. in the 3P/6P frequency range. Failing to recognize this early on is a major hazard for any project.
- Presence of vicious cycles in global design, e.g. the soft-stiff trap where an increase in structural capacity (to withstand the given loads) stiffens the tower and/or the main column, hence shifting the flexible frequencies upwards. This in turn reduces the 3P margin, resulting in a further load increase!
- Diverging design solutions to resolve local stress hotspots in fatigue or in strength. Typically: a structural design target fixation on strength checks (occurring when "fatigue will be treated later on") can subtly make the structure's philosophy unfit for withstanding fatigue.
- Compromises between fabrication requirements (weld quality, tolerances) and structural fatigue calculations & design hypotheses have huge impacts on fabrication and assembly duration and costs, and as such should be identified, discussed and rationalized early on. Especially considering serial production where these impacts will be highly repetitive.
- Higher cost (and hence material quantity) pressure on the project, requiring optimal scantling and fabrication choices.

1.3 Fatigue calculation process

So how does the marine designer respond to these new requirements? As soon as possible, they ought to cascade time-domain coupled loads into the substructure components to design, check, and optimize them against fatigue.

For a floating structure, this is a challenging undertaking because of the need to resolve stresses in complex parts of a moving body, with a high-enough mesh resolution. Rainflow counting can be performed only once stress time series are computed for relevant fatigue DLCs, in the number of tens, hundreds, or thousands depending on the design phase (see e.g. [5]). Moreover, a relatively high stress time series sampling frequency is dictated by the need to capture high-frequency cycles associated with vibrational aeroelastic responses making their way into the substructure.

At first sight, the resulting computational effort may look prohibitive: for a nominal stress study at mid-project stage, **tens of millions of time stamps need to be resolved over a mesh of tens of millions structural finite elements**. Not something one can generally envision doing in a regular FEA software tool, until TRUST (**TRU**e **S**tructural Analysis in **T**ime Domain) solution is introduced in 2022 [8].

2. TRUST algorithm for TD FEA

TRUST is a software developed by Front Energies, to obtain structural responses of FOW substructure in high-fidelity finite-element structural model in time domain with minimal computing time and resources. The FOW substructures are relatively stiffer than the other parts of FOW such as wind turbine, tower and mooring system and are typically modeled as linear elastic assumption. In the linear elastic FEA formulation, the equation of motion of the FOW substructure is given by

$$\boldsymbol{K u} = \boldsymbol{f}(\ddot{\boldsymbol{u}}, \dot{\boldsymbol{u}}, \boldsymbol{u}, \boldsymbol{t}) \tag{1}$$

The state variable, $\boldsymbol{u}$, is the nodal displacement vector including both linear and angular displacements at FE nodes. The internal strain and stress to be used for the fatigue assessment can be obtained from the nodal displacement vector, $\boldsymbol{u}$, finite-element approximation scheme adopted in FEA and the constitutive equation of the substructure material. The load on the substructure other than the internal load, $\boldsymbol{Ku}$, consists of the following three types of load patterns:

$$\boldsymbol{f} = \boldsymbol{f_p}(t) + \boldsymbol{f_b}(\ddot{\boldsymbol{u}}, \dot{\boldsymbol{u}}, \boldsymbol{u}) + \boldsymbol{f_S}(\ddot{\boldsymbol{u}}, \dot{\boldsymbol{u}}, \boldsymbol{u}, t) \tag{2}$$

where

- $\boldsymbol{f_p}$: Point (or nodal) load such as mooring and wind turbine tower connection force
- $\boldsymbol{f_b}$: Body force such as inertial and gravity force
- $\boldsymbol{f_S}$: Surface load such as hydrostatic and hydrodynamic force

The dimension of the displacement vector, $\boldsymbol{u}$, or DOF of FEA, N_{FE}, ranges from tens of thousands to millions, which makes it practically impossible to solve the equations in tens of millions of time steps in time domain. The time-domain motion of the substructure is rather obtained as part of the ILA, where only essential numbers of DOF of substructures are kept for the ILA.

Typically, rigid-body motion is assumed for the substructure in ILA considering higher stiffness of the substructure than other parts in FOW. In this case, the dimension of $\boldsymbol{u_{ILA}}$ is 6 and transformation matrix, $\boldsymbol{R}$, is a N_{FE} by 6 matrix with each column represents the nodal displacement of the 6 DOF rigid-body motion:

$$\boldsymbol{u}(t) = \boldsymbol{R u_{ILA}}(t) \tag{3}$$

For some FOW substructure design where the local elastic deformation is essential for the dynamics of FOW, the DOF higher than 6 can be used for the definition of $\boldsymbol{u_{ILA}}$ and $\boldsymbol{R}$. In this paper, TRUST algorithm limited to rigid-body-motion for ILA is described. For the general cases with higher DOF in ILA are addressed in [6].

Since rigid-body motion does not induce any internal load, the rank of the singular stiffness matrix, $\boldsymbol{K}$, is $N_{FE} - 6$, and

$$\boldsymbol{R^T K R u_{ILA}}(t) = \boldsymbol{0} \tag{4}$$

As a result, the displacement vector obtained from the ILA analysis and the transformation **(*3*)** should satisfy the following load-balance equation

$$\boldsymbol{R^T f}(\ddot{\boldsymbol{u}}, \dot{\boldsymbol{u}}, \boldsymbol{u}, \boldsymbol{t}) = \boldsymbol{0} \text{ with } \boldsymbol{u}(t) = \boldsymbol{R u_{ILA}}(t), \tag{5}$$

if the internal- and external loading corresponding to the rigid-body motion are consistently modeled in the equations of motion of FEA and ILA.

The total nodal displacement in addition to the rigid-body displacement is obtained by solving the following modified equation of motion:

$$(\boldsymbol{K} + \boldsymbol{K_c})\boldsymbol{u} = \boldsymbol{f}(\boldsymbol{R}\ddot{\boldsymbol{u}}_{\boldsymbol{ILA}}, \boldsymbol{R}\dot{\boldsymbol{u}}_{\boldsymbol{ILA}}, \boldsymbol{u}_{\boldsymbol{ILA}}, \boldsymbol{t}) \tag{6}$$

The addition of stiffness matrix, $\boldsymbol{K_c}$, makes the stiffness matrix non-singular if the following requirements are satisfied:

$$\det[\boldsymbol{R^T K_c R}] \neq \boldsymbol{0}, \tag{7}$$

The selection of $\boldsymbol{K_c}$ matrix is not unique but will not affect the solution of (6) as far as the rank of the matrix is 6 because of (1), (4) and (5). In typical TRUST analysis, the stiffness matrix, $\boldsymbol{K_c}$, is realized by putting linear springs at the fairleads (mooring line connection points).

The load-balance equation (5) can be used to check whether the ILA model is consistent with the FE model, and whether the evaluation of load components are made without error during the post processing of ILA results for the FEA input. However, most of FOW engineers use commercial FEA software and some of the load components are not available explicitly. Instead, we can use the resultant force from the springs that we put to add the

stiffness matrix, $\boldsymbol{K_c}$, in (6). By applying the matrix, $\boldsymbol{R^T}$, we obtain

$$\boldsymbol{R^T K_c u = R^T f(R\ddot{u}_{ILA}, R\dot{u}_{ILA}, u_{ILA}, t) = 0} \quad (8)$$

The left-hand side of (8) is no other than the resultant force and moment from the springs at fairleads that we put to form the stiffness matrix, $\boldsymbol{K_c}$. TRUST outputs the nodal displacements at the fairleads that can be used to calculate resultant force by simply multiplying the displacements and spring stiffness, and moments by multiplying moment arms to the resultant forces. These operations can be done not only to check the overall load balance but also the consistency between load components from FEA and ILA, which will be addressed in the next section.

3. LOAD PATTERNS, AMPLITUDES AND CONSISTENCY CHECK

The most time-consuming part of the TD FEA is solving (6) in each time step. In TRUST algorithm, the matrix equation (6) is not solved in each time step. TRUST utilized the following observations to minimize the number of solving FEA:

Fixed Geometry: The FEA for the structural response is made in the body-fixed coordinate.
Linear Structural Response: FE responses are linear to the internal and external loads.
Separability in Time and Space: All load components can be defined by load pattern (or spatial distribution) independent of time multiplied by load amplitude that depends only on the time.

The first two observations are intrinsic from the FEA formulation, but the last observation requires insights in understanding of the loads and ideas on how to separate the loads into spatial patterns and temporal amplitudes. The following subsections describe the insights and ideas built in TRUST algorithms. Also described are the requirements to assure consistent mapping of the loading from ILA to FEA for each load pattern.

3.1 Point Loads

In most of the ILA analysis software, such as OpenFAST and OrcaFlex, wind turbines and tower structure are modeled by nonlinear beam models and mass elements controlled by servos, under the external loads from turbulent wind field. This nonlinear mechanical system under the complicated wind loading, at the end, simply transmits 6 force (and moment) components to the substructure, in exchange for the 6 DOF motion at a single connection point. Mooring lines and IACs are also connected to the substructure in similar ways.

These load components are categorized as point loads with the following pattern and amplitudes defined in ILA and FEA:

Load pattern: 6 DOF force (4^{th} to 6^{th} components refers to moment in the sense of generalized force) with unit amplitude at the nodal point commonly shared by wind turbine tower and substructure.
Load amplitude: Time histories of 6 DOF connection force from ILA

Consistency requirements:

1. Same inertial coordinates of the connection point in ILA and FEA modeling.
2. Proper unit conversion between ILA and FEA. This requirement applies to all other load patterns and will not be repeated hereafter.

3.2 Body Force Loads

This load pattern applies to the distributed mass in FEA and concentrated mass in ILA. Inertia and gravity forces are under this category.

Load pattern in ILA: 6 by 6 mass (including moment of inertia in generalized sense) matrix

Load pattern in FEA: Distributed mass density of beam/shell/solid elements defined in input. In the case of ballast water, directional mass components are distributed as mass elements. At the end, they are discretized into N_{FE} by N_{FE} mass matrix.

Load amplitude: Time histories of 6 DOF acceleration and gravity in body-fixed coordinate

Consistency requirements:

1. Center of mass in ILA and FEA model should match each other.
2. Mass matrix in ILA, $\boldsymbol{M_{ILA}}$, and mass matrix in FEA, $\boldsymbol{M_{FE}}$, satisfies the following relationship:

$$\boldsymbol{M_{ILA} = R^T M_{FE} R} \quad (9)$$

During the design stage of FOW substructure, weight control engineers keep updating the weight information of the structural members, equipment, appendages and ballast. The above requirements can be satisfied if the same version of weight table is used for ILA and FE modeling. Most of the commercial FEA software, such as Nastran, also provides the center of mass and rigid-body mass matrix as a part of the analysis output, which can be used to check the requirements.

3.3 Surface Loads

Surface loads on the substructure are from hydrostatic and hydrodynamic loads on the wetted surface of the substructure. They consist of hydrostatic, linear hydrodynamic and nonlinear hydrodynamic forces.

3.3.1 Hydrostatic Load

Hydrostatic loads are from the integration of hydrostatic pressure on the wetted surface of the substructure. They consist of motion-independent buoyancy force at static position and motion-induced hydrostatic force represented by hydrostatic stiffness matrix multiplied by substructure motion.

Load pattern in ILA: buoyancy force and 6 by 6 hydrostatic stiffness matrix

Load pattern in FEA: hydrostatic pressure at stationary position (buoyancy) and additional hydrostatic pressure due to nodal displacement induced by unit 6 DOF rigid body motion.

Load amplitude: Buoyancy is given as a constant value. For the motion-induced hydrostatic load, time histories of the 6 DOF rigid-body motion are given as the load amplitudes.

Consistency requirements:

1. Substructure volume in ILA and FEA model match each other.
2. Resultant force from hydrostatic pressure by unit 6 DOF rigid-body motion in FEA should match each column in the hydrostatic stiffness matrix for ILA.

3.3.2 Linear Hydrodynamic Load

Linear hydrodynamic load consists of wave diffraction and radiation load. They are defined in the frequency domain.

3.3.2.1 Wave Diffraction Load

Load pattern in ILA: Wave diffraction force components in FD.

Load pattern in FEA: Wave diffraction pressure distribution in FD.

Load amplitude: Fourier transformation of wave elevation at a reference point. The reference point can be fixed at the mean horizontal position of the substructure or can move following the low-frequency motion of the substructure.

Consistency requirements:

1. Resultant force from linear diffraction pressure by unit wave amplitude in FEA should match with the 6 DOF the wave diffraction coefficients in ILA.
2. If substructure LF motion is considered in reference point of wave elevation, the definition of LF motion, such as cut-off frequency and low-pass filter scheme, should be consistent in ILA and FEA.

3.3.2.2 Radiation Load

Load pattern in ILA: Time-convolution kernel for the radiation force derived from the added mass and damping coefficients in FD.

Load pattern in FEA: Hydrodynamic pressure at due to unit 6 DOF rigid body motion in FD.

Load amplitude: Time histories of the 6 DOF rigid-body motion in ILA, Fourier coefficients of the 6 DOF motion in FEA.

Consistency requirements:

1. Resultant force from pressure by unit motion amplitude in FEA should match with the added mass and damping coefficients in FD.
2. Convolution integral of unit sinusoidal acceleration motion matches with corresponding added mass coefficients.
3. Convolution integral of unit sinusoidal velocity motion matches with corresponding wave damping coefficients.

3.3.3 Nonlinear Hydrodynamic Load

Nonlinear hydrodynamic load includes

1. Viscous drag load
2. Nonlinear Froude-Krylov force
3. Nonlinear diffraction force

They are mostly modeled by line load on Morison members in ILA. They are mapped to the FE elements aligned with the corresponding Morison members in ILA.

Load pattern in ILA: Unit nodal force on Morison elements.

Load pattern in FEA: Distributed traction on the FE elements aligned with the Morison members.

Load amplitude: Nodal force at Morison element nodes.

Consistency requirements:

1. Resultant force unit nodal force on Morison elements equals to the resultant force from corresponding traction distribution on FEA model.

3.3.4 Lumped Hydrodynamic Loads

Some of the hydrodynamic loads are not accounted for from the linear hydrodynamics theory for the linear frequency-domain hydrodynamic loads and Morison formula for the empirical viscous force. For instance, viscous flow around the floater induces additional inertial (added mass) and linear drag force. Those loads are estimated from the model test and/or CFD simulations. ILA software such as OpenFAST and OrcaFlex allows addition of those loads by

1. Directional added mass coefficient on Morison elements
2. Linear drag and damping force coefficient on Morison elements
3. Global drag and damping force coefficient applied at a specified point, usually at the center of mass of the FOW or substructure

Another type of nonlinear hydrodynamic load is the sum- and difference-frequency load from the second-order wave diffraction theory. Although the pressure distributions of these second-order loads are well-defined by the theory, evaluation of those loads on the FE elements is significantly time-consuming. Instead, simplified load distributions of these second-order loads are considered. There are several ways of simplification. One of them is using the distribution of inertial load, which is intrinsically embedded 'inertia relief' method. TRUST algorithm, however, uses pressure distribution on the wetted surface for the simplified load distribution of the second-order load components. The pressure distribution should have equivalent resultant force. Pressure distribution from the hydrostatic pressure components are chosen for this purpose.

The justification of the simplified pressure distribution for the second-order sum/difference frequency load is from the fact that these weak loads contribute mostly to the resonant substructure motion at low frequency, such as surge / sway / yaw motion, and at high frequency heave / pitch / roll motions of tension leg platform (TLP) substructure. The responses of substructure to these weak second-order loads are amplified due to low hydrodynamic damping at low- and high-frequency bands. The amplified rigid-body motion induces strong inertia and mooring load whose magnitudes are roughly inversely proportional to the damping ratio at the resonant frequencies. As a result, the structural loads from these second-order weak loads are not from second-order pressure but are mostly from the reaction inertia and mooring loads that only depend on the resultant force but not on the detail pressure distribution.

The third type of lumped hydrodynamic loads, global drag and damping force, uses the same pressure distribution as the second-order load components. For the first and second types of the lumped hydrodynamic loads, they are all treated as the same load distribution as the Morison drag load. Accordingly, the consistency requirements for the lumped hydrodynamic load follow the same requirements for the nonlinear hydrodynamic loads.

3.4 Evaluation of Structural Responses and Load Recovery

The evaluation of structural responses from the point and inertial loads are straightforward. The unit responses of point loads are obtained from the FE solutions of unit nodal forces at the nodes where the point loads are applied. Unit responses of body force loads are obtained from the FE solutions of unit body force or acceleration applied to all FE nodes with mass matrix, which are readily available in most of the commercial FEA software. Unit responses of surface loads are obtained from the solution of FEA with nodal pressure and traction values at wetted surface are applied. The final structural responses can be obtained by simply multiplying amplitudes of these load components to the unit structural responses, which are typically given by nodal-displacement and elemental-stress-tensor components. The unit structural responses are stored in an efficient data format to retrieve prior to the ILA and structural assessment. In TRUST operation, the data file where the unit structural responses of various load components are called 'Response Cartridge' and the blending of the unit responses by amplitudes of corresponding loads to obtain structural responses are called 'Response Printing'.

Some of the load components, such as radiation and wave diffraction load, are defined in frequency domain (FD, hereafter). The load patterns of these FD loads are obtained from FD hydrodynamic solvers such as WAMIT based on linear and second-order wave diffraction theory [9][10][11]. The structural responses, i.e., elemental stresses and nodal displacements, to these FD load components in unit amplitudes can be obtained from FE solver with corresponding pressure load input. The amplitudes of the FD loads, wave elevation and substructure motion, as transformed into FD amplitudes by FFT. Blending of the structural responses are done in FD similarly to the point and body-force loads in TD. The blended responses in FD are transformed back to TD by IFFT, to be combined with the other responses blended in TD.

One of the beauties of response printing by TRUST algorithm is that response printing can be done selectively for the structural assessment. For the fatigue assessment, for an example, stress can be printed only on the elements along the weld lines to evaluate fatigue damage as shown in FIGURE 2. For hot-spot fatigue assessment, the number of elements necessary for the fatigue assessment is even lower. For detailed structural model with millions of elements, the number of elements along the weld line reduces to tens of thousands and to a few thousands for hot spots. The selective response printing algorithm embedded in TRUST software makes the fatigue assessment of FOW extremely efficient. Damage counting of 30K elements from 1-hour ILA simulation, with 0.1 sec time step, takes less than 10 minutes in a typical Windows desktop. For the fatigue assessment with thousands of DLCs, TRUST operation is typically made in a HPC with enough CPUs and memory to perform the stress printing and damage counting with parallel operation. Fatigue assessment of 6,000 DLCs at 30K hotspots, for example, took less than 4 hours in the Frontera supercomputer in Texas Advanced Computing Center [12] using 40 nodes.

For each ILA simulation and TRUST operation, the load balance and recovery can be monitored from the nodal displacements of

the nodes where liner springs are applied to make the quasistatic system non-singular, and Equation ***(8)***.

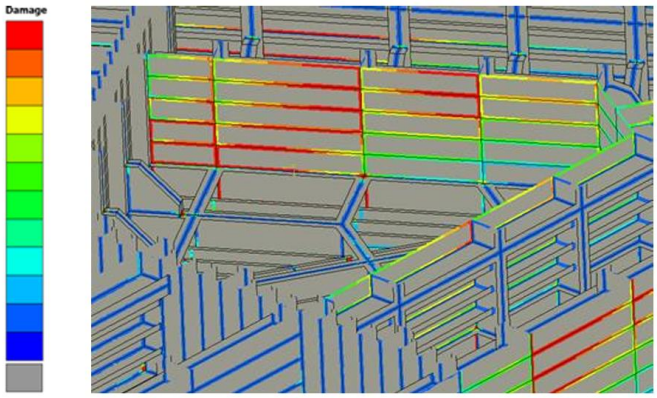

FIGURE 2: Fatigue Assessment along the Weld Lines of an FOW Internal Structure

4. CASE STUDY

4.1 FOW Model and Environmental Condition

As an application, structural analysis of a conventional semisubmersible FOW platform supporting a 15 MW turbine is performed utilizing both open-source (OpenFAST) and commercial (OrcaFlex) software for ILA. FD hydrodynamic coefficients and pressure distributions are calculated by WAMIT. FEA of the structural model is made by a commercial FEA software Siemens NX Nastran.

FIGURE *3* shows the overall view of the FOW rendered in an ILA software OrcaFlex. The dimensions, mass properties of the turbine and substructures are given in FIGURE 4 and TABLE *2*.

TABLE 3 shows the environmental condition selected for the case study. Water depth is 137 m.

TABLE 4 shows statistics of substructure motion from OrcaFlex and OpenFAST. There are minor differences in mean surge and heave. Other than that good agreement in motion statistics is found.

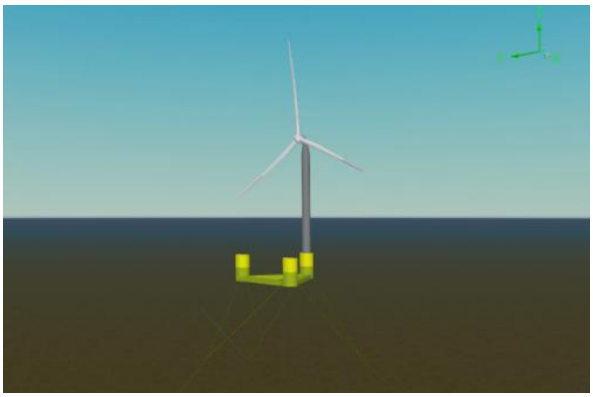

FIGURE 3: ILA Model of FOWT with 15MW IEA wind turbine

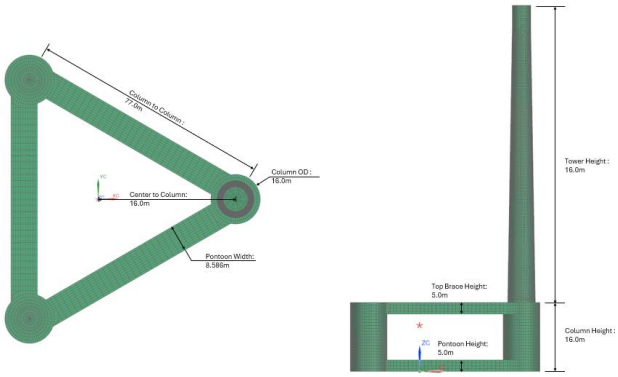

(a) Hull Configuration with Eccentric Tower Location

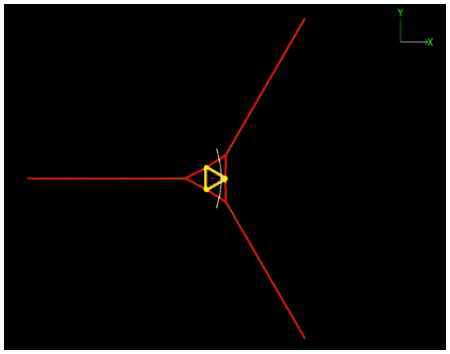

(b) YCCMS Mooring Configuration (Mooring lines - Red color)

FIGURE 4: Semisubmersible FOWT with 15MW IEA wind turbine

TABLE 2: Mass Distribution of 15MW FOWT

Items	Mass (MT)	x(m) from hull center	y(m) from hull center	z(m) from keel
RNA and Tower	2265	44.5	0.0	111.8
Substructure	5043	2.5	0.0	14.4
Ballast	9972	-11.4	0.0	3.0
Mooring vertical load	213	0.0	0.0	0.0
Total Displacement	17494	0.0	0.0	20.3

TABLE 3: Environmental Condition for DLC 1.6

Wind	
V	11.0 m/s
Dir	0 deg
Nac	0 deg
TI	14.0
Wave	
Hs	4.5 m
Tp	9.0 s
Gm	2.4
Dir	0 deg
Current	
V	0.8 m/s
Dir	0 deg

TABLE 4: Motion Statistics of OrcaFlex and OpenFAST

DOF	Software	Max	Min	Mean	Std.Dev.
Surge[m]	OrcaFlex	24.02	18.79	20.92	0.78
	OpenFAST	27.37	19.18	22.48	1.32
Sway[m]	OrcaFlex	-0.86	-0.92	-0.89	0.01
	OpenFAST	-0.06	-0.18	-0.10	0.02
Heave[m]	OrcaFlex	0.88	-1.09	-0.15	0.31
	OpenFAST	0.87	-1.37	-0.22	0.29
Roll[deg]	OrcaFlex	0.47	0.42	0.45	0.01
	OpenFAST	0.36	0.30	0.33	0.01
Pitch[deg]	OrcaFlex	4.24	2.47	3.57	0.28
	OpenFAST	4.40	2.44	3.60	0.27
Yaw[deg]	OrcaFlex	0.25	0.16	0.21	0.01
	OpenFAST	0.26	0.20	0.24	0.01

The FE model incorporates all primary structural components, including columns, pontoons, column top braces, and internal structures which contribute to the global stiffness of Hull. Primary members are modeled using 2D elements, while secondary stiffeners are represented with 1D elements. The total number of 2D elements is 37,500, and 1D elements are 25,774. The spring boundary conditions are applied at 6 mooring point locations. Ballast mass is modeled using distributed directional mass elements. The thickness distribution of the model is presented in FIGURE 5. The structural design of this model has been developed for a demonstration of TRUST software, and not for real applications. Some of the structural elements are purposely under designed for the demonstration purposes.

The FIGURE 6 and FIGURE 7 show the VM stress for each ILA dataset from OpenFAST and OrcaFlex.

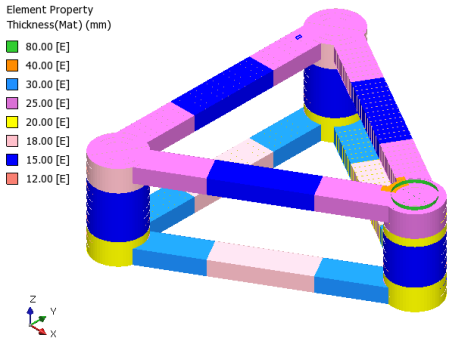

FIGURE 5: Thickness of FOWT Substructure Model

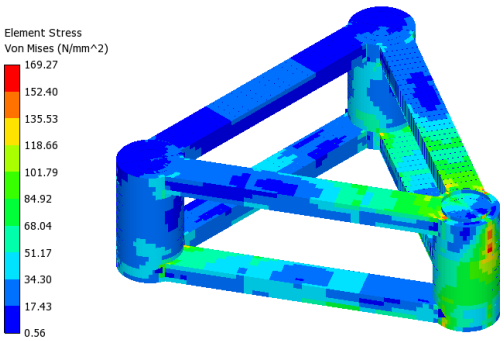

FIGURE 6: Structural Response - OpenFAST

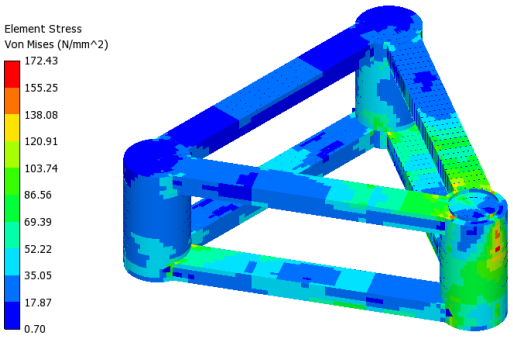

FIGURE 7: Structural Response – OrcaFlex

4.2 Consistency Check Results

4.2.1 Consistency-Check Strategy and Challenges

Consistency check has been performed by comparing resultant forces from the following load components:

- Wind load (point load)
- Inertial load (body-force load)
- Hydrostatic load (surface load)
- Wave diffraction load (surface load)

- Radiation load (surface load)
- Morison load (surface load)
- Mooring load (point load)

The most challenging load patterns to make ILA load to be fully recovered in the structural analysis are surface load, especially the wave diffraction and radiation load. These loads are evaluated in different software for the hydrodynamic coefficient in ILA and pressure distribution in FEA. In this case study, hydrodynamic coefficients are evaluated inside WAMIT software with higher-order panels, whereas pressure distributions are applied as nodal pressure at FE element nodes in Nastran. The finite element panels in FEA are typically finer than the panel used in WAMIT. Finer panel size of 2 m is used in WAMIT, rather than 5 m panel in typical analysis. This panel size assured good agreement in the resultant wave diffraction force in ILA and FEA, as shown in FIGURE *8*. In case of radiation force, additional care was necessary because of the following factors:

- Radiation force is evaluated by time convolution in TD ILA, whereas it is evaluated as Fourier series in TRUST.
- The time convolution integral in ILA by numerical quadrature in ILA, which might be less accurate than Fourier series in FD depending on the order of numerical quadrature.
- The added mass and damping coefficients are linearly interpolated for the frequencies other than the frequencies where the coefficients are provided as input for ILA and TRUST. This will affect the accuracy of the time-convolution kernel in ILA.

The last factor is resolved by increasing number of frequencies where the hydrodynamic coefficients are evaluated. Total 122 frequencies are resolved to achieve the satisfactory accuracy of the kernel, compared to 40 frequencies for typical ILA. Alternatively, higher-order interpolation scheme for the hydrodynamic coefficients can be used for the same purpose. The other factors have been resolved by improving numerical quadrature scheme in OpenFAST, source code of which is available, from trapezoidal rule to Simpson's rule. FIGURE 9 shows the comparison of radiation force with the improved scheme.

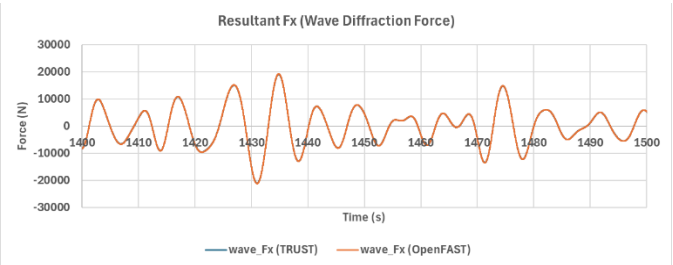

FIGURE 8: Wave Diffraction Force

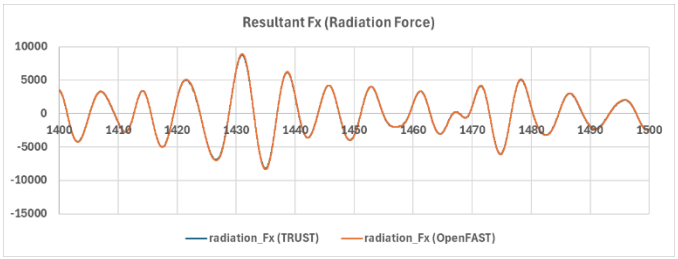

FIGURE 9: Radiation Force

With these improvements, more than 99% of the resultant force in ILA has been recovered in FEA by Nastran and TRUST. FIGURE 10 and FIGURE 11 show the time history of total resultant force and load recovery rate in the structural response by ILA results from OpenFAST and OrcaFlex, respectively. Statistics of the load balance in each load components and total load are given in TABLE 5 and TABLE 6 for OpenFAST and OrcaFlex, respectively. Load recovery rate of 99.8% is achieved in OpenFAST-based TD structural analysis. In case of OrcaFlex-based TD structural analysis, a slightly lower recovery rate of 99.2% is achieved. The tables also show the total resultant force from ILA, which is an indicator in load balance in ILA analysis. The higher total unbalanced load in OrcaFlex is partly due to uncertainties in understanding and interpreting the ILA result output from the software. Most unbalanced loads came from wave diffraction and radiation force. In the case of the open-source code OpenFAST, the detailed formulation and coding of each load component were traceable from the publicly available software, and also modified for better accuracy, if necessary, as in the case of radiation force improvement, which was not the case for OrcaFlex software. However, regardless of these differences, load recoveries from both software were satisfactory such that unrecovered load of less than 1% would not affect the structural assessment results.

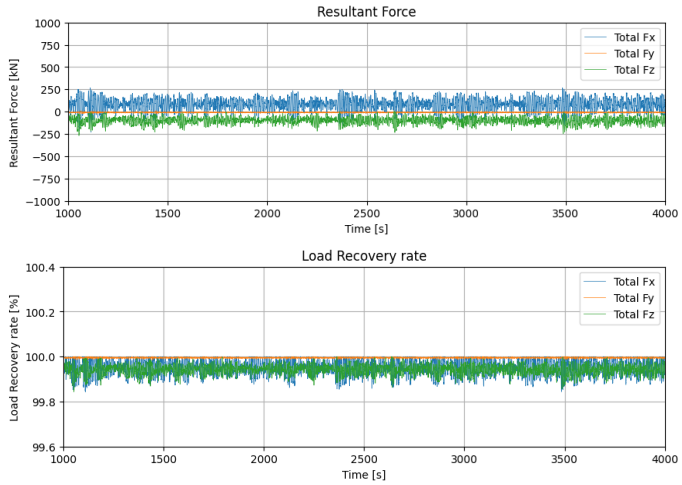

FIGURE 10: Total Load Balance – OpenFAST

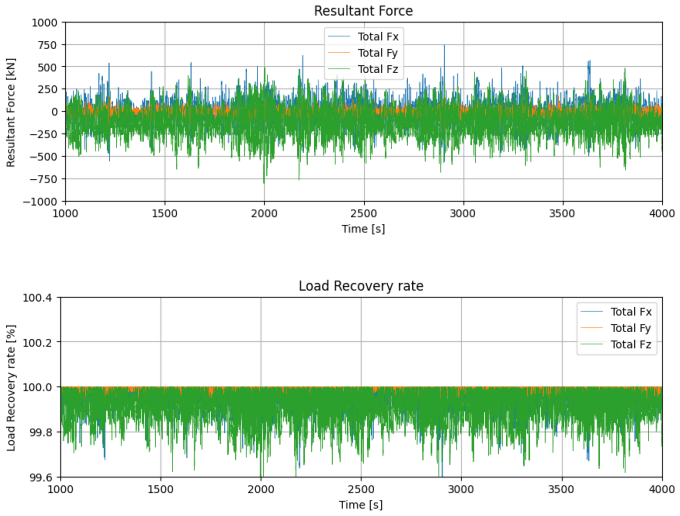

FIGURE 11: Total Load Balance – OrcaFlex

TABLE 5: Statistics of Resultant Force from OpenFAST

	Mean			STD			
	TRUST	OpenFAST	Difference	TRUST	OpenFAST	Difference	
Wind	3360.5	3360.5	0.0	596.4	596.4	0.0	
Wave	3.6	3.6	0.0	5931.8	5956.9	29.8	
Radiation	-1.0	-1.0	0.0	2623.0	2647.3	39.7	
Mooring	-2471.3	-2476.4	5.2	202.7	203.2	0.9	
Morison	713.4	709.5	3.9	645.4	641.9	3.6	
Inertial	9235.3	9247.9	-12.7	2941.3	2910.0	95.3	1hr
Hydrostatic	-10760.1	-10769.0	8.9	778.2	778.8	0.7	Extreme
Total	80.4	75.1	5.3	66.8	23.5	84.7	Value
Total/Disp	0.047%	0.044%	0.003%	0.039%	0.014%	0.049%	**0.18%**
Recovery	99.95%	99.96%	100.00%	99.96%	99.99%	99.95%	**99.82%**

TABLE 6: Statistics of Resultant Force from OrcaFlex

	Mean			STD			
	TRUST	OrcaFlex	Difference	TRUST	OrcaFlex	Difference	
Wind	2606.9	2606.9	0.0	615.8	615.8	0.0	
Wave	-2.6	-2.0	-0.6	5905.8	5908.4	110.7	
Radiation	0.5	10.2	-9.6	2659.5	2629.8	107.5	
Mooring	-2143.6	-2146.1	2.5	140.0	140.2	0.5	
Morison	514.6	576.7	-62.1	135.2	144.6	14.9	
Inertial	6864.4	6866.9	-2.6	2916.5	2916.3	0.8	1hr
Hydrostatic	-7980.5	-7987.1	6.6	828.2	828.9	0.7	Extreme
Total	-391.1	-74.5	-451.4	261.9	260.8	373.3	Value
Total/Disp	-0.23%	-0.04%	-0.26%	0.15%	0.15%	0.22%	**0.75%**
Recovery	99.8%	100.0%	99.7%	99.8%	99.8%	99.8%	**99.25%**

4.3 The Effect of Load Balance in Structural Response

To demonstrate the effect of load balance on fatigue damage, ILA and TRUST analyses of 110 fatigue bins representing DLC1.2 and DLC6.4 conditions in the Donghae Sea in Korea.

FIGURE 12 shows the overall fatigue damage distribution for fatigue bins under the balanced condition. FIGURE 13 shows fatigue damage from one of the fatigue bins. If the load balance is disrupted, accurate fatigue life prediction becomes challenging, as shown in FIGURE 13. Therefore, during FOWT structural and fatigue analysis, it is crucial to accurately transfer the time series loads calculated from ILA to structural model and, to ensure the load balance of model. The load imbalance results in stress concentration at the boundary condition, such as mooring point locations.

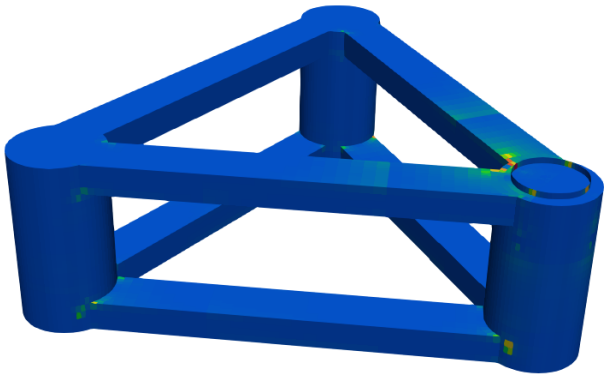

FIGURE 12: Fatigue Damage Distribution for Fatigue Bins

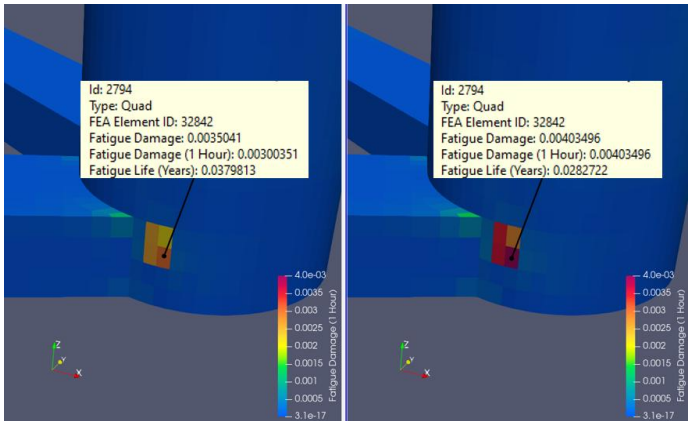

(a) Balanced Condition (b) Unbalanced Condition

FIGURE 13: Damage Difference on Mooring Point

5. CONCLUSIONS AND PATHFORWARD

TRUST algorithm that evaluates structural response of elastic FOW substructure in time domain from ILA with substructure modeled as a rigid body, is explained. Theoretical background to check consistency between ILA and FEA by resultant force from each model is shown.

Challenges in maintaining consistency between the two analyses models, and solutions to the challenges are presented and demonstrated. Load recovery of higher than 99% of displacement, or load unbalance less than 1% is achieved for a DLC1.6 case, where all wind, wave and current loads are applied.

The proposed TRUST algorithm has been applied to commercial FOW projects to evaluate safety of FOW substructure for various environmental conditions. Consistency between ILA and FEA/TRUST analysis is being monitored following the procedure described in this paper, as part of the QA of the engineering process involved.

As a concluding remark, the quasi-static assumption in the structural response, as followed in this paper, is only valid when ILA is made with rigid-body assumption. When the structural elasticity in substructure needs to be considered in ILA, dynamic structural responses need to be considered in FEA and structural assessments. In this case, the consistency requirement between ILA and FEA needs to be extended to DOF higher than 6. TRUST software is evolving in this direction [7].

REFERENCES

[1] IEC 61400-3-2 “Wind energy generation systems – Part 3-2: Design requirements for floating offshore wind turbines”.

[2] DNV-SE-0422 “Certification of floating wind turbines”.

[3] DNV-ST-0119 “Floating wind turbine structures”.

[4] BV NI 572 “Classification and Certification of Floating Offshore Wind Turbines”.

[5] Pineau H., Antonutti R., Martin A., and Guinot F., “Hyperbox method: a design-oriented selection of fatigue load cases for offshore wind turbines”, J. Phys.: Conf. Ser. 2875 012015, 2024.

[6] M.G., Baquet, A., Song, K.H., Kim, B.K., “Time-domain Response-based Structural Assessment of a FOWT – Part 1: Buckling and Ultimate Strength Assessment”, IOWTC2022-96497

[7] Yim, Y., Lee, H., Kyoung, J and Kim, J., “Effect of Structural Dynamics on Fatigue Damage in a Floating Wind Turbine Substructure,” OMAE2025-157502

[8] Lee, H.T., Kim, J.G., Kim, J.O., Shen, Z., Kyoung, J.H., Baquet, A., Lee, H.J., Kim, J.W., 2023, “An efficient time domain structural assessment of a floating wind turbine structure”, OMAE2023-108155.

[9] Wehausen, J. V. & Laitone, E. V. (1960), Flügge, S. & Truesdell, C. (eds.), "Surface Waves", Encyclopaedia of Physics, 9, Springer Verlag: 446–778

[10] Newman, J.N., 1977, “Marine Hydrodynamics,” MIT Press

[11] Lee, C.H., 1995, “WAMIT Theory Manual, www.wamit.com

[12] Dan Stanzione, John West, R. Todd Evans, Tommy Minyard, Omar Ghattas, and Dhabaleswar K. Panda. 2020. Frontera: The Evolution of Leadership Computing at the National Science Foundation. In Practice and Experience in Advanced Research Computing (PEARC ’20), July 26–30, 2020, Portland, OR, USA. ACM, New York, NY, USA, 11 pages. https://tacc.utexas.edu/systems/frontera/